

## Impurity Transport Study by means of Tracer-Encapsulated Solid Pellet in LHD

N. Tamura<sup>1</sup>, K. V. Khlopenkov<sup>1</sup>, S. Sudo<sup>1</sup>, S. Kato<sup>1</sup>, V. Yu. Sergeev<sup>2</sup>,  
S. Muto<sup>1</sup>, K. Sato<sup>1</sup>, H. Funaba<sup>1</sup> and LHD experimental groups<sup>1</sup>

<sup>1</sup>National Institute for Fusion Science, 322-6 Oroshi-cho, Toki, Gifu 509-5292, Japan

<sup>2</sup>State Technical University, Polytechnicheskaya 29, St.Petersburg, 195251 Russia

### 1. Introduction

In order to realize a practical fusion reactor, impurity particle transport is still one of the important issues. This study has been done intensely by means of an impurity injection. Conventional methods for the impurity injection, however, have essential disadvantages, such as a broad source profile of the injected impurities and an ambiguity of the total amount of those. In order to solve these problems and to promote impurity particle transport studies, a tracer-encapsulated solid pellet (TESPEL) [1] has been developed [2] and in recent Large Helical Device (LHD) experiments, the TESPEL injection has been implemented [3, 4]. TESPEL consists of polystyrene (-CH (C<sub>6</sub>H<sub>5</sub>) CH<sub>2</sub>-) as an outer shell (typically ~ 0.7 mm  $\phi$ ) and tracer particles as an inner core (typically ~ 0.2 mm size). It is a unique characteristic of TESPEL to be able to produce a both poloidally and toroidally localized particle source as a tracer of a quantity that is well known. Moreover, the flexible choice of the tracer particle is one of the important characteristics with the object of the investigation of the Z-dependence of impurity transport. In LHD, metallic impurity accumulation has been found only in hydrogen discharges with a line-averaged electron density  $n_{e\_bar}$  around  $2.0 \times 10^{19} \text{ m}^{-3}$  [5]. In this paper, the quantitative transport properties of this phenomenon are investigated by means of the TESPEL with a titanium (Ti) tracer.

### 2. Experimental apparatus

The Large Helical Device (LHD) is the world's largest heliotron device having a superconducting  $l/m = 2/10$  helical coils and 3 pairs of superconducting poloidal coils. The experiments subjected to this work were conducted under conditions of major radius  $R_{ax} = 3.6 \text{ m}$ , a magnetic field  $B_t = 2.75 \text{ T}$ ,  $n_{e\_bar} = (0.3\text{-}3.5) \times 10^{19} \text{ m}^{-3}$  and the electron temperature  $T_e = (1.8\text{-}2.9) \text{ keV}$ . A TESPEL is injected from the outboard side of LHD by means of the pneumatic pipe-gun technique. In order to obtain the deposition feature of TESPEL, the ablation light of the TESPEL injected into LHD plasma is observed by CCD cameras and photo-multiplier tubes with corresponding interference filters for shell and tracer. In case of the Ti tracer, several Ti micro-balls (with 80-100  $\mu\text{m}$  diameter) have been filled inside the TESPEL. The total amount of Ti particle was varied approximately in the  $(0.5\text{-}3) \times 10^{17}$  range. The behavior of emission lines from the highly ionized Ti tracer impurity, Ti  $K\alpha$  ( $E_{\text{He-like}} \sim 4.7 \text{ keV}$ ) and Ti XIX ( $\lambda = 16.959 \text{ nm}$ ), have been observed by an X-ray pulse height analyzer (PHA) and a vacuum ultra violet (VUV) spectrometer, respectively. Two PHA systems have been used. One system (PHA20) is

installed on the equatorial plane of LHD Port 2-O to observe the LHD plasma central chord. Another system (PHARD), which has 3 channels, is done at Port 2.5-L to observe the radial profile of X-ray emissions. The energy resolution of the PHA system is approximately 300 ~ 400 eV. Thus, the measured Ti K $\alpha$  emission by these systems contains Ti K $\alpha$  line emissions from several charge states.

### 3. Experimental results and Discussions

Figure 1 shows the dependence of the decay time of Ti K $\alpha$  emission measured by the PHA20 on the line-averaged electron density for balanced NBI heated plasmas with the TESPEL injection. The decay time of Ti K $\alpha$  increases gradually as the value of  $n_{e\_bar}$  increases from  $0.3 \times 10^{19} \text{ m}^{-3}$  to  $1.9 \times 10^{19} \text{ m}^{-3}$ . There are points above  $3.0 \times 10^{19} \text{ m}^{-3}$ , which have a considerably longer decay time. This is consistent qualitatively with the experimental results by the observations of behavior of an intrinsic impurity [5].

In order to estimate the transport coefficients, the impurity transport code, MIST [6] has been used. A cylindrical symmetry is assumed. The radial particle flux  $\Gamma_i$  for the  $i$ -th charge state ion is modeled by a simple diffusive-convective model:

$$\Gamma_i = -D_i(r)\partial n_i/\partial r + V_i(r)n_i$$

, where  $n_i$  is the density of the impurity,  $D_i(r)$  is the radial diffusion coefficient and  $V_i(r)$  is the convective velocity, respectively. In our study, the diffusion coefficient is assumed to be a constant in time and space and the convective velocity term is represented as  $V_i = -C_v(2rD/a^2)$ , where  $C_v$  is the convection parameter,  $a$  is the averaged minor radius of plasma (here,  $a = 63 \text{ cm}$ ), and those are common among all charge states.

As seen in figure 2, the trial and error analysis with the MIST indicates that the observed behavior of the emissions of the highly ionized Ti tracer at the value of  $n_{e\_bar} = 1.8 \times 10^{19} \text{ m}^{-3}$  is well described by the value of  $D = 1000 \text{ cm}^2/\text{sec}$  and  $V = 0 \text{ cm}/\text{sec}$ , that is, the no convection. Here, the intensity of Ti K $\alpha$  emission measured by the PHA20 is normalized by the value at the time when the Ti K $\alpha$  emission reaches a maximum.

On the other hand, at the value of  $n_{e\_bar} = 3.5 \times 10^{19} \text{ m}^{-3}$ , the temporal evolution of the emissions of Ti K $\alpha$  and Ti XIX is in fairly good agreement with the case of  $D = 600 \text{ cm}^2/\text{sec}$  and  $V(a) = -76 \text{ cm}/\text{sec}$  (see figure 3).

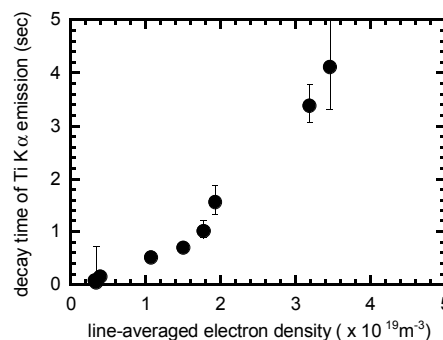


Figure 1. The dependence of the decay time of Ti K $\alpha$  emission on the line-averaged electron density in the case of balanced NBI heated LHD plasmas.

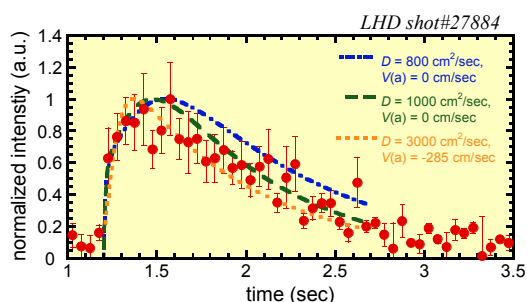


Figure 2. Comparison of normalized temporal evolution of Ti K $\alpha$  emission (closed circles) measured by the PHA20 with those calculated by MIST with several sets of  $D$  and  $V$  at the value of  $n_{e\_bar} = 1.8 \times 10^{19} \text{ m}^{-3}$  (the blue dash-dotted line:  $D = 800 \text{ cm}^2/\text{sec}$ ,  $V = 0 \text{ cm}/\text{sec}$ , the green dashed one:  $D = 1000 \text{ cm}^2/\text{sec}$ ,  $V = 0 \text{ cm}/\text{sec}$ , the dotted one:  $D = 3000 \text{ cm}^2/\text{sec}$ , the orange convective velocity at the plasma edge  $V(a) = -285 \text{ cm}/\text{sec}$ ).

From the point of view of global behavior, the Ti impurity transport with  $n_{e\_bar} = 3.5 \times 10^{19} \text{ m}^{-3}$  can be explained with the value of  $D = (300 \sim 900) \text{ cm}^2/\text{sec}$  and  $V(a) = -(19 \sim 114) \text{ cm}/\text{sec}$ . In this case, the inward convection should be taken into account.

We investigate the parameter space to where the plasma with the inferred convection belongs. The parameter space shown in figure 4 is defined by the electron density and the electron temperature at the peripheral region of LHD plasma ( $\rho = 0.7$ ). The solid line in figure 4 indicates the boundary between the Banana-plateau (BP) regime and the Pfirsch-Schlüter (PS) regime. For the simplicity, this boundary is calculated with the following assumption. Firstly, the collision between the Ti impurity ion and the bulk plasma ion has been only considered. Secondly, a dominant charge state of the Ti impurity ion is helium-like. As seen in figure 4, the data point with the value of  $n_{e\_bar} = 3.5 \times 10^{19} \text{ m}^{-3}$  belongs to the PS regime. On the other hand, the case of  $n_{e\_bar} = 1.8 \times 10^{19} \text{ m}^{-3}$  belongs to the BP regime. In order to examine the experimentally deduced convective velocities, the neoclassical expressions of the radial impurity flux for axisymmetric devices are utilized for the both regimes, although it might be arguable that the one for axisymmetric devices can be utilized for non-axisymmetric devices in case of the BP regime. The radial impurity flux in the BP regime for axisymmetric devices is given by [7]

$$\Gamma_{BP} = -D_{imp} (n_{imp}'/n_{imp} + 3T_{imp}'/2T_{imp} - Z_{imp}n_i'/n_i - 3Z_{imp}T_i'/2T_i) n_{imp} \quad (1)$$

, where the subscript of 'imp' and 'i' denotes the impurity ion and the bulk plasma ion, respectively. The last two terms have an important role in the case of the higher Z impurities. The inward flux could be driven by the negative  $n_i'$  and  $T_i'$  in this case. In case of the PS regime, the impurity flux is written as [7]

$$\Gamma_{PS} = -D_{imp} (n_{imp}'/n_{imp} - T_{imp}'/2T_{imp} - Z_{imp}n_i'/n_i + Z_{imp}T_i'/2T_i) n_{imp} \quad (2)$$

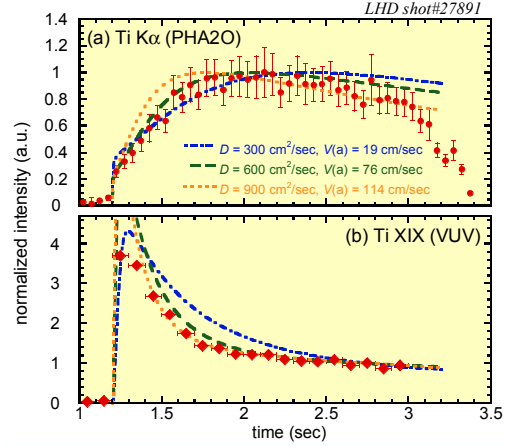


Figure 3. Comparison of normalized temporal evolution of (a) Ti K $\alpha$  emission (closed circles) measured by the PHA20 and (b) Ti XIX emission (closed diamond) done by the VUV spectrometer with those calculated by MIST with several sets of  $D$  and  $V$  at the value of  $n_{e\_bar} = 3.5 \times 10^{19} \text{ m}^{-3}$  (the blue dash-dotted line:  $D = 300 \text{ cm}^2/\text{sec}$ ,  $V(a) = -19 \text{ cm}/\text{sec}$ , the green dashed one:  $D = 600 \text{ cm}^2/\text{sec}$ ,  $V(a) = -76 \text{ cm}/\text{sec}$ , the orange dotted one:  $D = 900 \text{ cm}^2/\text{sec}$ ,  $V(a) = -114 \text{ cm}/\text{sec}$ ). The balanced NBI was terminated at  $t = 3.3 \text{ sec}$ .

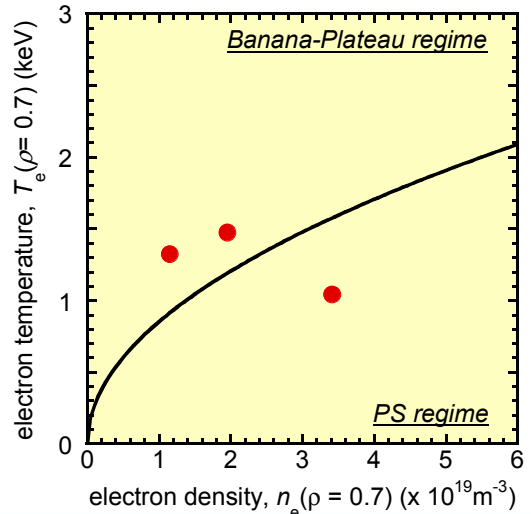


Figure 4. Data points for the transport analysis using MIST in the balanced NBI plasmas on the parameter space defined by  $n_e$  and  $T_e$  at the normalized averaged minor radius  $\rho = 0.7$ . The solid line indicates the boundary between the Banana-Plateau (BP) regime and Pfirsch-Schlüter (PS) regime on the assumption that the collision between the Ti impurity ion and the bulk plasma ion (proton) have been only considered and the dominant charge state of the Ti impurity ion is taken as helium-like. The data point with the value of  $n_{e\_bar} = 3.5 \times 10^{19} \text{ m}^{-3}$  belongs to the PS regime.

In this regime, the last density term could drive the inward impurity flux. On the other hand, the last temperature term could induce the outward one. In any case, the scale length of  $n_i$  and  $T_i$  should cause the convective flux toward the center or the edge. Thus, assuming that  $n_e \sim n_i$  and  $T_e \sim T_i$ , the scale lengths of  $n_e$  and  $T_e$  are estimated. And then the neoclassical convective velocities in the case with  $n_{e\_bar} = 1.8 \times 10^{19} \text{ m}^{-3}$  and with  $n_{e\_bar} = 3.5 \times 10^{19} \text{ m}^{-3}$  are calculated with the estimated values of the  $n_e$  and  $T_e$  scale lengths. In case of  $n_{e\_bar} = 1.8 \times 10^{19} \text{ m}^{-3}$ , the convective velocity at  $\rho = 0.7$ , which deduced from the MIST analysis, 0 cm/sec, agree with the neoclassical one at  $\rho = 0.7$ ,  $(-101.6 \pm 128.7)$  cm/sec, within the range of the error. On the other hand, in case of  $n_{e\_bar} = 3.5 \times 10^{19} \text{ m}^{-3}$ , the neoclassical value at  $\rho = 0.7$ ,  $(52.7 \pm 46.6)$  cm/sec has the opposite sign (the outward), compared with the experimentally deduced one at  $\rho = 0.7$ ,  $-53.3$  cm/sec. Therefore, the estimated convective velocity cannot be explained in case of  $n_{e\_bar} = 3.5 \times 10^{19} \text{ m}^{-3}$  solely by the effects of the pure neoclassical impurity transport and the effect of some kind, which originates the inward flux, should be taken into account.

#### 4. Conclusions

The quantitative transport properties of Ti impurity on LHD plasmas heated by the balanced NBI was investigated by means of the TESPEL injection. The fairly longer decay time of the line emissions from highly ionized Ti tracer was observed above the value of  $n_{e\_bar} = 3.0 \times 10^{19} \text{ m}^{-3}$ . As a result of the MIST analysis for the higher density case, the inward convection is required to account for the experimental results, even though the absolute inward convective velocity is less than around 100 cm/sec. The comparison between the experimentally deduced convective velocities and the ones calculated by the neoclassical impurity transport has been performed. The inferred rise of the inward convection cannot be explained solely by the pure neoclassical impurity transport.

#### Acknowledgments

The authors would like to thank Professor O. Motojima for his continuous encouragement of this work and all of the technical staffs of NIFS for their support. This work is partly supported by Grant-in-Aid for Scientific Research (B) No. 10480109 and grant No. L00537 of Japan Society for the Promotion of Science (JSPS).

#### References

- [1] Sudo S 1993 *J. Plasma Fusion Res.* **69**, 1349
- [2] Khlopenkov K *et al* 1998 *Rev. Sci. Instrum.* **69**, 3194
- [3] Tamura N *et al* 2001 *J. Plasma Fusion Res. SERIES* **4**, 442
- [4] Sudo S *et al* 2002 *Plasma Phys. Control. Fusion* **44**, 129
- [5] Nakamura Y *et al* 2001 *Proc. 28<sup>th</sup> EPS Conf. Controlled Fusion Plasma Phys.* **25A**, 1481 (Funchal, Portugal)
- [6] Hulse R A 1983 *Nuclear Technology/Fusion* **3**, 259
- [7] Fussmann G *et al* 1991 *Plasma Phys. Control. Fusion* **33**, 1677